Implementation of a Novel Efficient Multiwavelet Based Video Coding Algorithm

Sudhakar Radhakrishnan and Jayaraman Subramaniam
Department of Electronics and Communication Engineering, PSG College of Technology, India.

Abstract: *The recent explosion in digital video storage and delivery has presented strong motivation for high performance video compression solutions. An efficient video compression technique must preserve the trade-off between compression ratio and the quality of the video. The performance of existing image and video coding standards generally degrade at low bit-rates because of the underlying block based Discrete Cosine Transform (DCT) scheme. Over the past decade, the success of wavelets in solving many different problems has contributed to its unprecedented popularity. Due to implementation constraints scalar wavelets do not posses all the properties which are needed for better performance in compression. New class of wavelets called 'Multiwavelets' which posses more than one scaling filters overcomes this problem. The objective of this paper is to develop an efficient compression scheme for the video stream by fast motion estimation algorithms up to half pixel accuracy as in newest international standard, ITU-T H.264/AVC, and to obtain better quality and higher compression ratio through multiwavelet transform and embedded coding of multiwavelet coefficients through Set Partitioning In Hierarchical Trees algorithm (SPIHT).*

Keywords: *video compression, quantization, prediction, entropy coding, multiwavelets, scaling functions.*

Received April 7, 2006; Accepted December 1, 2006

1. Introduction

Video compression is now essential for applications such as transmission and storage. Video coding has evolved through the development of the ISO/IEC MPEG-1, MPEG-2 and ITU-T H.261, H.262 and H.263 video coding standards [10, 20], and later enhancements of H.263 known as H.263+ and H.263++. Throughout this evolution, continued efforts have been made to maximize coding efficiency.

The performance of these coders generally degrades at low bit-rates mainly because of the underlying block-based Discrete Cosine Transform (DCT) [11] scheme. In the DCT the input image needs to be blocked. So correlation across the block boundaries is not eliminated resulting in noticeable and annoying blocking artifacts. More recently, the wavelet transform has emerged as a cutting edge technology, within the field of image compression [2, 4, 7, 18]. Wavelet-based coding provides substantial improvements in picture quality at higher compression ratios. For better performance in compression, filters used in wavelet transforms should have the property of orthogonality, symmetry, short support and higher approximation order. Due to implementation constraints scalar wavelets do not satisfy all these properties simultaneously [16]. New class of wavelets called 'Multiwavelets' which posses more than one scaling filters [3, 1] overcomes this problem.

Thus multiwavelets offer the possibility of superior performance and high degree of freedom for image processing applications, compared with scalar wavelets. Multiwavelets can achieve better level of performance than scalar wavelets with similar computational complexity. In this paper, an efficient algorithm is presented for motion estimation using fast approach algorithms [9, 6, 3, 5]. A comparison of the best known multiwavelets is made to the best known scalar wavelets. Both quantitative and qualitative measures of performance are examined for several videos and images. This paper is organized as follows: Section 2 highlights some key technical features of our design that enable improved operation. Section 3 provides the basic theory of multiwavelets. Section 4 presents the encoding and decoding process of the proposed video coding design. Results and discussions are presented in section 5 and finally conclusions are drawn in the section 6.

2. Design Feature Highlights

- *Multiple reference picture motion compensation:* prediction in MPEG-2 and its predecessors use only one previous picture to predict the values in an incoming picture. The new design extends upon the enhanced reference picture selection technique found in H.263++ and H.264 to enable efficient coding by allowing an encoder to select, for motion compensation purposes, among a three frames that have been decoded and stored in the decoder.
- *Variable block-size motion compensation with small block sizes*: our algorithm supports more

flexibility in the selection of motion compensation block sizes than any previous standard, with a minimum luma motion compensation block size, as small as, 4x4. Our algorithm supports block sizes of 16x16, 8x8 and 4x4.

- *Fast algorithms for motion estimation*: to reduce the time taken to find the best matching block among three reference frames fast estimation algorithm, new cross diamond search algorithm is used. To reduce the complexities involved in interpolations processing, *fast two step* methods for half pixel accuracy motion estimation is used.
- *Image based transform*: all the existing standards for both image and video coding except JPEG2000 uses DCT based transform. In the wavelet based transforms there is no need to block the image. Wavelet based coding provides substantial improvement in picture quality at higher compression ratios mainly due to the better energy compaction property of wavelet transforms.
- *Adaptive quantization method*: the choice of a good quantizer depends on the transform that is selected, since the properties possessed by the coefficients from the transformation stage depend on the transform used. For evaluating the effectiveness of the wavelet or multiwavelet transform for coding images or videos at low bit rates, an effective quantization and embedded coding of coefficients has been realized using modified SPIHT.
- *Predictive coding of motion vectors*: encoding a motion vector for each partition can take a significant number of bits, especially if small partition sizes are chosen. So much of the compressed data will consist of motion vectors. The efficiency with which they are coded has a great impact on the compression ratio. To reduce the number of bits required to code, the motion vectors are predicted from the previously coded motion vectors and the difference is encoded using the variable bit rate coding.

3. Multiwavelets

Multiwavelets is defined using several wavelets with several scaling functions [3, 17]. Multiwavelets have several advantages in comparison with scalar wavelet [15]. The features such as compact support, orthogonality, symmetry, and high order approximation are known to be important in signal processing. A scalar wavelet can not possess all these properties at the same time [14]. On the other hand, a multiwavelet system can simultaneously provide perfect reconstruction while preserving length (orthogonality), good performance at the boundaries (via linear-phase symmetry), and a high order of approximation (vanishing moments) [17, 16]. Thus multiwavelets offer the possibility of superior performance and high degree of freedom for image processing applications, compared with scalar wavelets.

When a multiresolution analysis is generated using multiple scaling functions and wavelet functions, it gives rise to the notion of multiwavelets [13, 17, 16]. A multiwavelet with 'r' scaling functions and 'r' wavelet functions is said to have multiplicity 'r'. When $r = 1$, one scaling function and one wavelet function, the multiwavelet system reduces to the scalar wavelet system.

Multiwavelets differ from scalar wavelet systems in requiring two or more input streams to the multiwavelet filter bank [21]. Corresponding to each multiwavelet system, there is a matrix-valued multi-rate filter bank. A multiwavelet filter bank has "taps" that are $N \times N$ matrices. The 4-coefficient symmetric multiwavelet filter bank whose low pass filter is given by the four $N \times N$ matrices named C. Unlike a scalar 2-band Para unitary filter bank, the corresponding high pass filter specified by the four $N \times N$ matrices named D, cannot be obtained simply as an "alternating flip" of the low pass filter; the wavelet filters D must be designed. The resulting N-channel, $N \times N$ matrix filter bank operates on N input data streams, filtering them into *2N* output streams, each of which is down sampled by a factor of 2. This is shown in Figure 1. Each row of the multi-filter is a combination of N ordinary filters, each operating on the separate data stream.

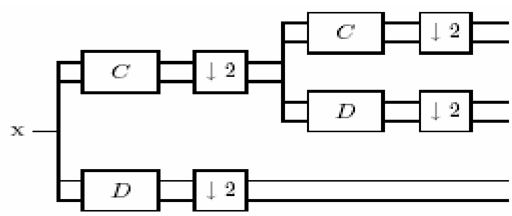

Figure 1. Multi-rate filter bank.

4. Encoding and Decoding Process

All luma and chroma samples are either encoded using transform coding or temporally predicted and the resulting prediction residual is encoded using transform coding. Each block is transformed using discrete Multiwavelet transform, and the transform coefficients are quantized and encoded using modified SPIHT and coding methods. Figure 2 shows a block diagram of the proposed video coding algorithm.

4.1. Inter Frame Prediction

The prediction signal for each predictive-coded MxN luma block is obtained by displacing an area of the corresponding reference picture, which is specified by a translational motion vector [9, 6] and a picture reference index.

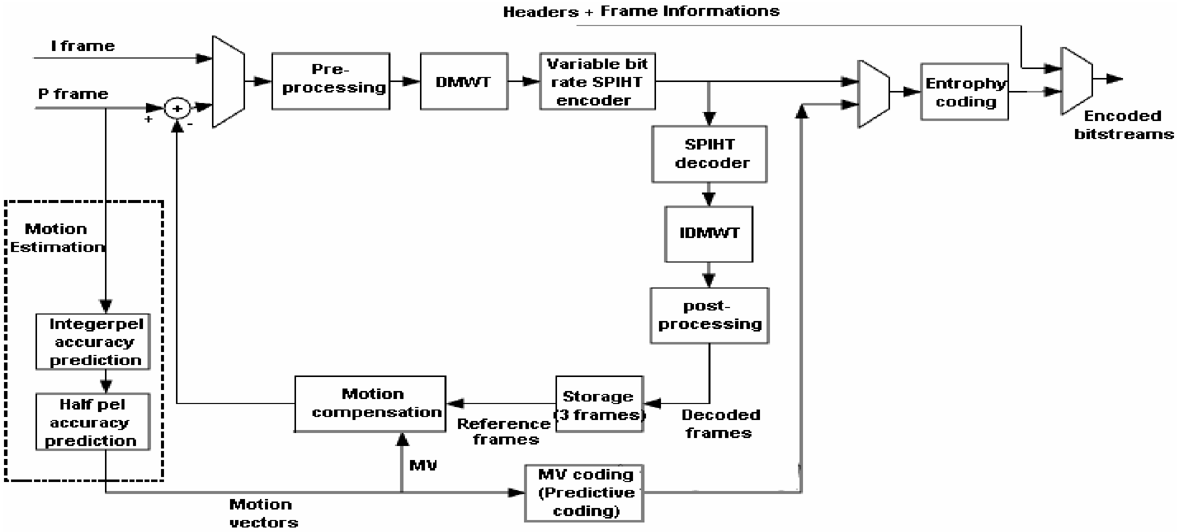

Figure 2. Proposed video coding algorithm.

Thus, if the macroblock is coded using four 8x8 partitions and each 8x8 partition is further split into four 4x4 partitions, a maximum of sixteen motion vectors may be transmitted for a single '*P*' macro block. The accuracy of motion compensation is in units of one half of the distance between luma samples. In case the motion vector points to an integer sample position, the prediction signal consists of the corresponding samples of the reference picture; otherwise the corresponding sample is obtained using interpolation to generate non-integer positions. The prediction values at half-sample positions are obtained by applying a one-dimensional 6-tap FIR filter horizontally and vertically. The syntax supports multi-picture motion compensated prediction. That is, more than one prior coded picture can be used as reference for motion-compensated prediction. Figure 3 illustrates the concept. In addition to the motion vector, also picture reference parameters are transmitted. Multi-frame motion-compensated prediction requires both encoder and decoder to store the reference pictures used for inter prediction in a multi-picture buffer. The decoder replicates the multi-picture buffer of the encoder according to memory management control operations specified in the bit stream. The reference index parameter is transmitted for each motion-compensated 16x16, 8x8, or 4x4 luma block. Motion compensation for 4x4 blocks uses the same reference index for prediction of all four blocks within the 8x8 region.

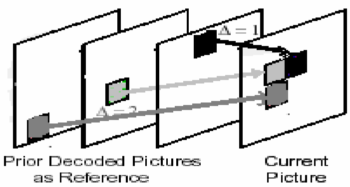

Figure 3. Multi-reference frame motion compensation.

4.1.1. Motion Estimation Algorithms

Full Search Algorithm (FSA) performs searching all the possible points in a search window exhaustively. Due to the high intensive computation required for the full search algorithm many fast motion algorithms has been proposed [9] over the last two decades to give a faster estimation with similar block distortion compared to the full search method. Many fast search algorithms[5] such as, Logarithmic Search Algorithm (LSA), Three Step Search (TSS), New Three Step Search (NTSS), Four Step Search (FSS), New Four Step Search (NFSS), Diamond Search (DS), Cross Search (CS), Cross Diamond Search (CDS), Predictive Search Algorithm (PSA) and Multilevel Successive Elimination Algorithm (MSEA) have been proposed.

The main aim of these FSAs is to reduce the number of search points in the search window and hence the computations. One of the most important assumptions of all fast motion estimation algorithm is 'error surface is monotonic', i.e., Block Distortion Measure (BDM) is the least at the center or the global minima of the search area and it increases monotonically as the checking point moves away from the global minima. *New Cross Diamond Search algorithm (NCDS)* which is based on the cross centre biased distribution characteristics [6] is employed here. The NCDS algorithm introduced half-way stop technique to achieve speed-up. Instead of performing all the steps as in three steps Search or four step search, searching process is terminated at any step based on some criteria. The bit streams are further compressed by using entropy. Encoder and decoder to store the reference pictures used for inter prediction in a multi-picture buffer. The decoder replicates the multi-picture buffer of the encoder according to memory management control frame motion-compensated prediction requires both operations specified in the bit stream.

4.1.2. The NCDS Algorithm

The main difference between NCDS [2] and CDS is that the first 2 steps of NCDS are keeping a small cross shaped pattern which is saving the number of search point for stationary or quasi-stationary blocks. The various steps and the analysis of the algorithm are given below.

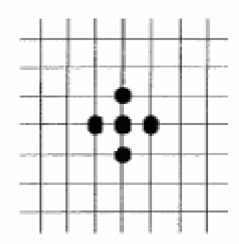

a. Small cross shape

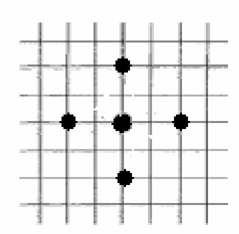

b. Large crosses shape

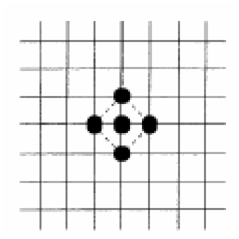

c. Small diamond shape

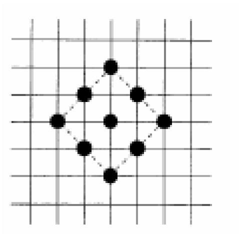

d. Large Diamond shape.

Figure 4. Searching patterns in NCDS algorithm.

Step 1: a minimum BDM is found from the 5 search points of the Small Cross-Shaped Pattern (SCSP) shown in Figure 4-a located at the center of search window. If the minimum BDM point occurs at the center of the SCSP, the search stops and the minimum BDM point found is the final solution for the motion vector. Otherwise, go to next step.

Step 2: with the vertex, i.e., minimum BDM point, in the first SCSP as the center, a new SCSP is formed. If the minimum BDM point occurs at the center of this SCSP, the search stops and the new minimum BDM point found is the final solution for the motion vector. Otherwise go to next step.

Step 3: the three unchecked outermost search points of the central LCSP are checked, in which the step is trying to guide the possible correct direction for the subsequent steps. And then go to next step.

Step 4: a new Large Diamond Search Pattern (LDSP). Is formed, as shown in Figure 4-c by repositioning the minimum BDM point found in previous step as the center of the LDSP. If the new minimum BDM point is at the center of the newly formed LDSP, then go to next step for converging the final solution; otherwise, this step is repeated.

Step 5 is the Converging step: With the minimum BDM point in the previous step as the center, a SDSP is formed. The new minimum BDM point is found from 4 search points of the SDSP. The new minimum BDM point found is the final solution for the motion vector.

Example for the NCDS algorithm is shown in Figure 5. The searching points in the each step are shown with different symbols. The minimal MAD point in each step is shown with grey color and also the direction of the convergence is shown by arrow marks. The final minimum MAD point which is the motion vector for the current block is (3, 2).

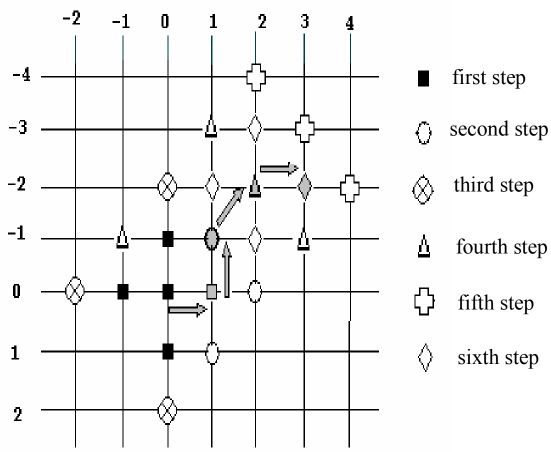

Figure 5. Example of NCDS algorithm.

4.2. Transform Coding

Similar to previous video coding standards, this algorithm utilizes transform coding of the *I*-frame as well as prediction residual. However, the transformation is applied to entire image; a discrete Multiwavelet transform is used.

4.2.1. Iteration Decomposition

Since multiwavelets decomposition produce two low pass subbands (if the number of scaling function is two) and two high pass subbands in each dimension [1, 8], the organization and statistics of multiwavelets subbands differ from the scalar wavelet case. During a single level of decomposition using a scalar wavelet transform, the 2-D image data is replaced with four blocks corresponding to the subbands representing either low pass or high pass in both dimensions.The Multiwavelets decomposition subbands are shown in Figure 6.

L_1L_1	L_1L_2	L_1H_1	L_1H_2
L_2L_1	L_2L_2	L_2H_1	L_2H_2
H_1L_1	H_1L_2	H_1H_1	H_1H_2
H_2L_1	H_2L_2	H_2H_1	H_2H_2

Figure 6. Multiwavelet decomposition subband structure for 1-level decomposition.

The multiwavelets used here have two sets of scaling coefficients and two sets of multiwavelets coefficients. Since the multiple iterations over the low pass data are desired, the scaling coefficients for the two channels are stored together. Likewise, the wavelet coefficients for the two channels are also stored together. For example, the subband labeled L_1H_2 corresponds to data from the second channel high pass filter in the horizontal direction and the first channel low pass filter in the vertical direction. In practice, more than one level of decomposition is performed on the image. Successive decompositions are performed on the low pass coefficients from the previous stage to further reduce the number of low pass coefficients. Since the low pass coefficients contain most of the original signal energy, this iteration process yields better energy compaction. Experiments indicate that three levels are sufficient for multiwavelets with gains in the PSNR diminishing rapidly with decomposition depth increasing above 3.

A single level of decomposition with a symmetric-anti symmetric multiwavelets is roughly equivalent to two levels of wavelet decomposition. Thus a 3-level multiwavelet decomposition effectively corresponds to 6-level scalar wavelet decomposition. Since tests indicate that the improvement from depth 5 to depth 6 for scalar wavelets is negligible. A 3-level multiwavelet decomposition can be considered comparable to 5-level scalar wavelet decomposition. The multiwavelet decompositions iterate on the low pass coefficients from the previous decompositions, as shown in Figure 7. In the case of scalar wavelets, the low pass quarter image is a single subband. But when the multiwavelet transform is used, the quarter image of low pass coefficients is actually a 2x2 block of subbands (the L_1L_1, L_1L_2, L_2L_1 and L_2L_2 subbands in Figure 6). Due to the nature of the preprocessing and symmetric extension method, data in these different subbands becomes inter mixed during iteration of the multiwavelets transform. The inter mixing of the multiwavelet low pass subbands leads to suboptimal results.

<table>
<tr><td>L_1L_1</td><td>L_1L_2</td><td>L_1H_1</td><td>L_1H_2</td><td rowspan="2">L_1H_1</td><td rowspan="2">L_1H_2</td></tr>
<tr><td>L_2L_1</td><td>L_2L_2</td><td>L_2H_1</td><td>L_2H_2</td></tr>
<tr><td>H_1L_1</td><td>H_1L_2</td><td>H_1H_1</td><td>H_1H_2</td><td rowspan="2">L_2H_1</td><td rowspan="2">L_2H_2</td></tr>
<tr><td>H_2L_1</td><td>H_2L_2</td><td>H_2H_1</td><td>H_2H_2</td></tr>
<tr><td colspan="2">H_1L_1</td><td colspan="2">H_1L_2</td><td>H_1H_1</td><td>H_1H_2</td></tr>
<tr><td colspan="2">H_2L_1</td><td colspan="2">H_2L_2</td><td>H_2H_1</td><td>H_2H_2</td></tr>
</table>

Figure 7. Multiwavelet decomposition subband structure for 2-level decomposition.

4.3. Coding of Multiwavelet Coefficients Using Modified SPIHT Algorithm

For evaluating the effectiveness of the Multiwavelet transform for coding images or videos at low bit rates, an effective quantization and embedded coding of coefficients [8, 12] has been realized. Some of the embedded coding schemes are embedded image coding using zero trees of Wavelet coefficients (EZW), and SPIHT. The SPIHT coder [12] is a powerful image compression algorithm that produces an embedded bit stream from which the best reconstructed images can be obtained at various bit rates. This algorithm improves the perceptual quality of the image at all the bit rates. The Modified SPIHT algorithm for Multiwavelet differs from the ordinary SPIHT [12] algorithm by the way in which the subsets are partitioned and significant information is conveyed which is shown in Figure 8. A tree structure, called spatial orientation tree, defines the spatial relationship on the hierarchical pyramid. Figure 9 shows how spatial orientation tree is defined for Multiwavelet coefficients. The following sets of coordinates are used to present the new coding method:

O (i, j): Set of coordinates of all offspring of node(i, j)
D (i, j): set of coordinates of all descendants of node (i, j)
H (i, j): set of coordinates of all spatial orientation tree roots (nodes in the highest pyramid level)
L (i, j): D (i, j) – O (i, j) (all descendents except the offspring).

4.3.1. Modified SPIHT Coding Algorithm

All the steps of the modified SPIHT coding algorithm are same except the initialization process. The modified SPIHT algorithm can be summarized as follows:

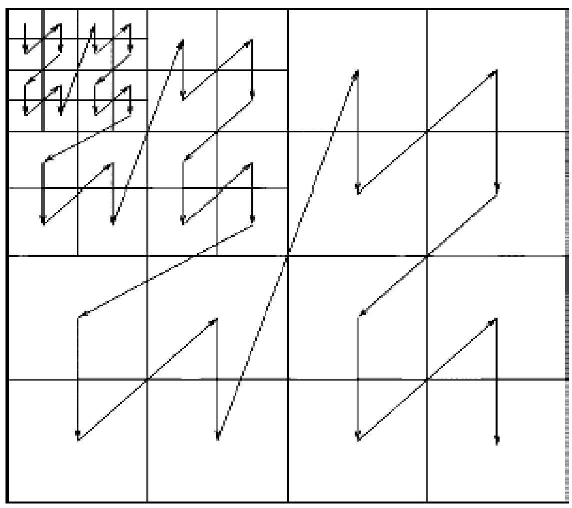

Figure 8. Scanning and quantization order of sub images of Multiwavelet decomposition.

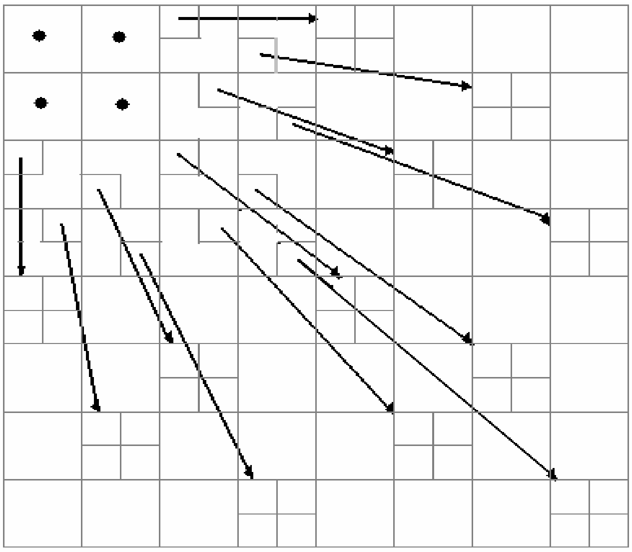

Figure 9. Spatial orientation tree of multiwavelet decomposition.

Since the order in which the subsets are tested for significance is important, in a practical implementation the significance information is stored in the ordered list called (a) List of Insignificant Sets (LIS), (b) List of Insignificant Pixels (LIP), (c) List of Significant Pixels (LSP). In all lists each entry is identified by a coordinate (i, j), which in the LIP and LSP represents individual pixels, and in the LIS represents either the set D (i, j) or L (i, j). To differentiate between them, we say that a LIS entry is of type A. If it represents D (i, j), and of type B if it represents L (i, j)

Initialization:

$$n = \lfloor log_2(max_{(i,j)})\{|C_{i,j}|\}\rfloor \qquad (1)$$

where $C_{i,j}$ is called wavelet coefficient.

Add the coordinates of H in which the scanning order of subbands as shown in figure 11, to the LIP and only those with descendents also to the LIS, as type A entries in the same order. For example the order of scanning of subbands is 'L_1L_1', 'L_2L_1', 'L_1L_2', 'L_2L_2', 'H_1L_1', 'H_2L_1', 'H_1L_2', 'H_2L_2', 'L_1H_1', 'L_2H_1', 'L_1H_2', 'L_2H_2', 'H_1H_1', 'H_2H_1', 'H_1H_2' and 'H_2H_2'.

A. Sorting Pass:

For each entry (i,j) in the LIP do:

a) Output S_n (i, j)

b) If S_n (i, j) =1, then move (i, j) to the LSP and output the sign of $C_{i,j}$

For each entry (i, j) in the LIS do:

a) If the entry is of type A then

(i) Output S_n (D(i, j))

(ii) If S_n (i, j) =1 then for each (k,l) ∈O(i, j) do:

(1) Output S_n(k,l)

(2) If S_n(k,l) =1 then add (k,l) to the LSP and output the sign of $C_{k,l}$

(3) If S_n(k,l) =0 then add (k,l) to the end of LIP

(4) If $L_{i,j} \neq \phi$ then move (i, j) to the end of the LIS as entry of type B, and go to step 2 otherwise remove entry from the LIS.

b) If the entry is of type B then

(i) Output S_n(L(i, j))

(ii) If S_n (L (i,j))=1 then

(1) add each (k,l) ∈O(i,j) to the end of the LIS as entry of type A

(2) remove (i,j) from the LIS

B. Refinement Pass:

For each entry (i, j) in the LSP except those included in the last sorting pass (i.e. with the same n), output the nth most significant bit of /Ci,j/.

C. Quantization Step Update:

Decrement the value of n by 1 and go to sorting pass if n is not less than 0.

5. Results and Discussion

The various types of videos namely 'Clarie', 'Football', 'Dancer', Tennis', and 'Flower' were taken for the comparisons of the results. The Multiwavelet filters [8, 16] used in this work were "GHM" pair of multifilters, Chui-Lian orthogonal multifilter "Cl", orthogonal symmetric/antisymmetric multifilter "Sa4", and Cardinal 2-balanced orthogonal multifilter "Cardbal2" and the corresponding prefilters used were 'Ghmap', 'Clap', 'Sa4ap', and 'Id', respectively. The PSNR results and the compression ratios for various videos using different Multiwavelets are shown in Table 1.

Table 1. Comparison of PSNR (in dB) values and compression ratios for various videos using various multiwavelets.

Video		Multiwavelets			
		Ghm	Cl	Sa_4	$Cardbal_2$
Claire	PSNR	40.89	41.48	*41.59*	41.11
	CR	52.43	*52.93*	52.33	52.09
Football	PSNR	32.7	32.74	*32.75*	32.74
	CR	47.56	47.46	*47.72*	47.53
Dancer	PSNR	40.65	38.45	*40.67*	38.19
	CR	46.39	*47.01*	46.73	46.54
Tennis	PSNR	34.67	*34.78*	34.67	34.68
	CR	56.63	*57.56*	57.44	58
Flower	PSNR	30.1	30.19	*30.25*	30.16
	CR	17.67	*23.36*	23.1	22.77

The results are tabulated for five videos using different Multiwavelets with the I-frame rate as bpp=1.0 and residual rate as bpp=0.2. The same experiment is repeated using wavelet based filters. The wavelets used in this experiment are “Haar”, “D4” [2, 3, 4] (Daubechies 4 coefficient orthogonal scalar filter bank), “La8” [2, 3, 4] (Daubechies 8 coefficient least asymmetric orthogonal scalar filter bank), “B9/7” (9/7 coefficient symmetric biorthogonal scalar filter bank). The results of the PSNR and CR using wavelet based coder are depicted in Table 2.

The highest value of PSNR and CR value for different videos using multiwavelets are highlighted in Table 1. Similarly ‘B9/7’ wavelet performs better than other wavelets are highlighted in Table 2.

Table 2. Comparison of PSNR (in dB) values and compression ratios for various videos using various wavelets.

Video		Wavelets			
		Haar	D_4	La_8	$B_{9/7}$
Claire	PSNR	33.89	34.32	35.24	*36.35*
	CR	41.43	40.93	40.33	*41.09*
Football	PSNR	28.43	29.74	29.32	*29.83*
	CR	45.56	45.36	45.57	*45.53*
Dancer	PSNR	35.65	36.15	36.37	*36.77*
	CR	45.39	45.01	45.73	*45.54*
Tennis	PSNR	32.32	32.23	33.67	*33.55*
	CR	48.05	47.56	47.44	*48.63*
Flower	PSNR	27.1	27.29	27.25	*27.57*
	CR	15.67	21.36	21.1	*21.77*

On comparing Tables 1 and 2, it is clearly indicated that multiwavelets outperform wavelets by having a PSNR improvement of roughly 2-5 dB with the increase in compression ratio on all the videos experimented. The results in Table 1, shows that the “Sa4” multifilters give the better PSNR values compared to other filters for all videos.

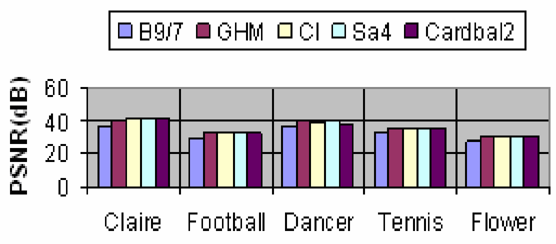

Figure 10. Comparison of PSNR values for different videos using wavelet (B9/7) and different multiwavelets.

The “Cl” multifilter gives the better compression ratios compared to other filters for all videos except the ‘Football’ video which has many objects and motions.

Table 3. Comparison of PSNR (in dB) values for coding of residuals by various multiwavelets at the different rate.

Rate	Video	Multiwavelets			
		Ghm	Cl	Sa4	Cardbal2
Bpp =0.1	Dancer	43.84	43.91	43.84	*43.92*
	Claire	44.77	45.71	*45.91*	45.04
	Tennis	38.7	38.83	38.85	*39.08*
	Football	36.34	36.43	*36.47*	36.46
	Flower	*34.4*	33.59	33.51	33.54
Bpp =0.2	Dancer	44.09	44.14	44.08	*44.16*
	Claire	44.8	45.75	*45.96*	45.09
	Tennis	38.76	35.09	*38.9*	36.45
	Football	36.45	36.55	*36.6*	36.56
	Flower	*34.46*	33.65	33.57	33.59

All the filters give better performance for the ‘Claire’ and ‘Dancer’ videos and very less compression ratio for the ‘Flower’ video with an acceptable quality.

Even the rate for coding the coefficients is fixed for all videos; the compression ratio for ‘Flower’ video is less compared to the other videos due to extra bits taken for coding the motion vectors, since this video contains more motions in the entire frame. Since the prediction residual has more redundancy and is to be coded with lesser rate than that of I- frame is evident from the results shown. Figure 10 shows the comparative results between best wavelet ‘$B_{9/7}$’ among the other wavelets taken for experiment and other multiwavelets. Table 3 shows the performance of each multifilter on the residuals of the predicted frame and how the residuals can be coded efficiently at the low bit rates.The performance of each multifilters on different videos is shown in Figures 11 and 12. The first four frames of the reconstructed ‘Elaine’ and ‘Dancer’ video are shown in Figures 13 and 14.

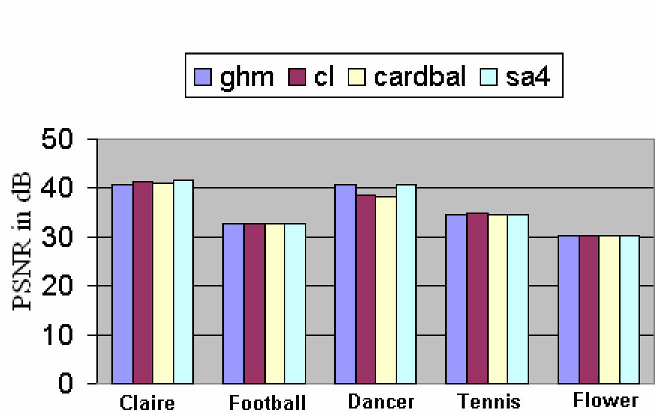

Figure 11. Comparison of PSNR values for different videos using different multiwavelets.

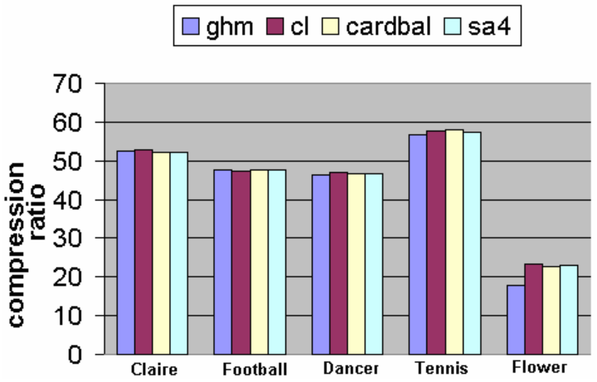

Figure 12. Comparison of CR for different videos using different multiwavelets.

Figure 13. Reconstructed first four frames of "CLAIRE" video.

Figure 14. Reconstructed first four frames of "DANCER" video.

6. Conclusion

This design is based on conventional block-based motion-compensated hybrid video coding concepts, but with some important differences relative to prior standards. Some of the important differences are (1) enhanced motion prediction capability, (2) use of discrete multiwavelet transform and (3) adaptive quantization Scheme. When used all together, the features of the new design provide a compression ratio of approximately 50 for equivalent perceptual quality relative to the performance of prior standards. Using multiwavelets and SPIHT coding, better compression ratio and quality is obtained compared to wavelets and quantization methods used in prior standards. Since this algorithm is still under research, time of execution for both multiwavelets and wavelets are not shown.

References

[1] Cotronei M., Lazzaro D., Montefusco L., and Puccio L., "Image Compression Through Embedded Multiwavelet Transform Coding," *IEEE Transactions on Image Processing,* vol. 9, no. 2, pp. 184-189, 2000.

[2] DeVore R., Jawerth B., and Lucier B., "Image Compression Through Wavelet Transforms Coding," *IEEE Transactions on Information Theory*, Special Issue on Wavelet Transforms and Multiresolution Signal Analysis, vol. 38, no. 2, pp. 719-746, 1992.

[3] Geronimo J., Hardin D., and Massopust P., "Fractal Functions and Wavelet Expansions Based on Several Functions," *Journal of Approximation Theory*, vol. 78, pp. 373-401, 1994.

[4] Hwang W. and Mallat S., "Singularity Detection and Processing with Waveletes," *IEEE Transactions Information Theory*, vol. 38, pp. 617-643, 1992.

[5] Koya T., Iinuma K., Hirano A., Iyima Y., and Ishi-guro T., "Motion-Compensated Inter-Frame Coding for Video Conferencing," *in Proceedings of the National Telecommunication Conference (NTC81)*, New Orleans, LA, pp. G531-G535, 1981

[6] La C., Po L., and Cheung C., "A New Cross-Diamond Search Algorithm for Fast Block Matching Motion Estimation," *IEEE Transactions on Image Processing*, vol. 9, no. 2, pp. 287-290, 2000.

[7] Mallat S., *A Wavelet Tour of Signal Processing*, Academic Press, New York, 1998.

[8] Martin M. and Bell A., "New Image Compression Techniques Using Multiwavelets and Multiwavelet Packets," *IEEE Transactions on Image Processing,* vol. 10, no. 4, pp. 500-511, 2001.

[9] Rao A. and Raghavan M., *Fast Motion Estimation Algorithms Computation and Performance Trade-Offs*, Academic Press, New York, 2003.

[10] Rao K. and Hwang J., *Techniques, Standards for Image, Video, and Audio Coding*, Prentice Hall, PTR, 1996.

[11] Rao K. and Yip P., *Discrete Cosine Transforms - Algorithms, Advantages, Applications,* Academic Press, 1990.

[12] Said and Pearlman W., "A New, Fast and Efficient Image Codec Based on Set Partitioning in Hierarchical Trees," *IEEE Transactions Circuits Systems Video Technology*, vol. 6, no. 3, pp. 243-250, 1966.

[13] Soman K. and Ramachandran K., *Insight into Wavelets from Theory to Practice*, Prentice Hall Of India, New Delhi, 2004.

[14] Strang G. and Nguyen T., *Wavelets and Filter Banks*, Wellesley, MA:Wellesley-Cambridge Press, 1995.

[15] Strang G. and Strela V., "Short Wavelets and Matrix Dilation Equations," *IEEE Transactions Signal Processing,* vol. 43, pp. 108-115, 1995.

[16] Strela V., Heller P., Strang G., Topiwala P., and Heil C., "The Application of Multiwavelet Filter Banks to Image Processing," *IEEE Transactions on Image Processing,* vol. 8, no. 4, pp. 548-563, 1999.

[17] Tham J., Shen L., Lee S., and Tan H., "A General Approach for Analysis and Application of Discrete Multiwavelet Transforms," *IEEE Transactions Signal Processing*, vol. 48, pp. 457-464, 2000.

[18] Vetterli M. and Kovacevic J., *Wavelets and Subband Coding,* Englewood Cliffs, Prentice Hall, 1995, http:/ /cm.bell-labs.com/ who/ jelena/ Book/ home.html.

[19] Vetterli M. and Strang G., "Time-Varying Filter Banks and Multiwavelets," *Sixth IEEE DSP Workshop*, Yosemite, pp. 223-226, 1994.

[20] Wiegand T., Sullivan G., Bjontegaard G., and Luthra A., "Overview of the H.264 / AVC Video Coding Standard," *IEEE Transactions on Circuits System Video Technology*, pp. 243-250, 2003.

[21] Wonkookim and Chung C., "On Preconditioning Multiwavelet System for Image Compression," *International Journal of Wavelets Multiresolution and Information Processing*, vol. 1, no. 1, pp. 51-74, 2003.

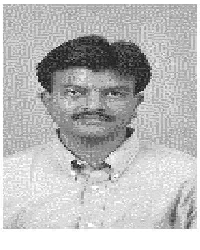

Sudhakar Radhakrishnan received the BE in electronics and communication engineering from Madras University in the year 1990 and ME in communication systems from Thiagarajar College of Engineering, Madurai in the year 2001. His research areas include image compression beyond wavelets, i.e., wavelet footprints, multiwavelets, contourlet transform. He has published five papers in various international journals. He is working as senior lecturer in deptartment of ECE, PSG College of Technology for the past three years. He has nearly 12 years of teaching experience. His areas of interest include digital signal processing, digital image processing, signals & systems, adaptive signal processing and statistical signal processing.

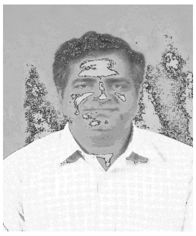

Jayaraman Subramaniam received the BE in electronics and communication engineering and ME and PhD, from PSG College of Technology. He has 28 years of teaching experience. He is currently the professor and head of ECE Department in PSG College of Technology. He has published more than 35 papers in journals and conferences. His areas of interest include DSP, statistical signal processing, multirate signal processing and adaptive signal processing, non linear signal processing, multidimensional signal processing.